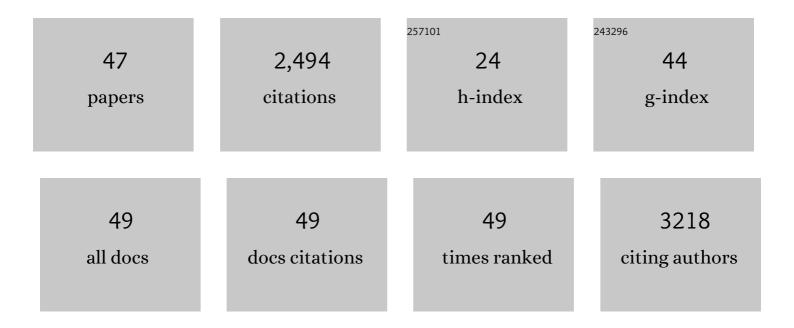
Lin Chen

List of Publications by Year in descending order

Source: https://exaly.com/author-pdf/8566847/publications.pdf Version: 2024-02-01



LIN CHEN

#	Article	IF	CITATIONS
1	Effect of bentonite on the stability of fresh cement slurry. Journal of Sustainable Cement-Based Materials, 2022, 11, 345-352.	1.7	1
2	The hangman effect boosts hydrogen production by a manganese terpyridine complex. Chemical Communications, 2022, 58, 5128-5131.	2.2	8
3	Hydrophobization Engineering of the Air–Cathode Catalyst for Improved Oxygen Diffusion towards Efficient Zinc–Air Batteries. Angewandte Chemie - International Edition, 2022, 61, .	7.2	72
4	A bio-inspired mononuclear manganese catalyst for high-rate electrochemical hydrogen production. Dalton Transactions, 2021, 50, 4783-4788.	1.6	8
5	Mechanically Strong, Thermally Healable, and Recyclable Epoxy Vitrimers Enabled by ZnAl-Layer Double Hydroxides. ACS Sustainable Chemistry and Engineering, 2021, 9, 2580-2590.	3.2	42
6	Electrostatic Interactions Accelerating Water Oxidation Catalysis via Intercatalyst O–O Coupling. Journal of the American Chemical Society, 2021, 143, 2484-2490.	6.6	25
7	Highâ€Temperature Nitridation Induced Carbon Nanotubes@NiFeâ€Layeredâ€Doubleâ€Hydroxide Nanosheets Taking as an Oxygen Evolution Reaction Electrocatalyst for CO ₂ Electroreduction. Advanced Materials Interfaces, 2021, 8, 2101165.	1.9	13
8	Multipleâ€Site Concerted Proton–Electron Transfer in a Manganeseâ€Based Complete Functional Model for [FeFe]â€Hydrogenase. Angewandte Chemie - International Edition, 2021, 60, 25839-25845.	7.2	9
9	Introducing electrostatic interaction into Ru(bda) complexes for promoting water-oxidation catalysis. Journal of Molecular Structure, 2021, 1242, 130745.	1.8	1
10	Strong, tough and healable elastomer nanocomposites enabled by a hydrogen-bonded supramolecular network. Composites Communications, 2020, 22, 100530.	3.3	24
11	Multilayered epoxy composites by a macroscopic anisotropic design strategy with excellent thermal protection. Journal of Materials Science, 2020, 55, 14798-14806.	1.7	4
12	Bioinspired Design of Positioned Amine Assists Hydrogen Evolution from Neutral Water by Nickel Tripyridineâ€Ðiamine. ChemCatChem, 2020, 12, 3853-3856.	1.8	1
13	A Janus Fe‣nO ₂ Catalyst that Enables Bifunctional Electrochemical Nitrogen Fixation. Angewandte Chemie - International Edition, 2020, 59, 10888-10893.	7.2	192
14	Synthesis, structure and electrocatalytic H2-evoluting activity of a dinickel model complex related to the active site of [NiFe]-hydrogenases. Chinese Chemical Letters, 2020, 31, 2483-2486.	4.8	4
15	A Janus Fe‣nO ₂ Catalyst that Enables Bifunctional Electrochemical Nitrogen Fixation. Angewandte Chemie, 2020, 132, 10980-10985.	1.6	57
16	Polyethylene glycol supported by phosphorylated polyvinyl alcohol/graphene aerogel as a high thermal stability phase change material. Composites Part B: Engineering, 2019, 179, 107545.	5.9	82
17	Entropy-driven catalytic reaction-induced hairpin structure switching for fluorometric detection of uranyl ions. Mikrochimica Acta, 2019, 186, 653.	2.5	13
18	Zinc doping induced differences in the surface composition, surface morphology and osteogenesis performance of the calcium phosphate cement hydration products. Materials Science and Engineering C, 2019, 105, 110065.	3.8	34

Lin Chen

#	Article	IF	CITATIONS
19	Structure-controlled Co-Al layered double hydroxides/reduced graphene oxide nanomaterials based on solid-phase exfoliation technique for supercapacitors. Journal of Colloid and Interface Science, 2019, 549, 236-245.	5.0	61
20	Controlled Self-Assembled NiFe Layered Double Hydroxides/Reduced Graphene Oxide Nanohybrids Based on the Solid-Phase Exfoliation Strategy as an Excellent Electrocatalyst for the Oxygen Evolution Reaction. ACS Applied Materials & Interfaces, 2019, 11, 13545-13556.	4.0	61
21	Controllable designing of superlattice units of tiled structure and standing structure as efficient oxygen evolution electrocatalyst: self-assembled graphene and hydroxide nanosheet. Journal of Materials Science, 2019, 54, 9034-9048.	1.7	8
22	Proximity ligation assay induced hairpin to DNAzyme structure switching for entropy-driven amplified detection of thrombin. Analytica Chimica Acta, 2019, 1064, 104-111.	2.6	18
23	Selective electroreduction of dinitrogen to ammonia on a molecular iron phthalocyanine/O-MWCNT catalyst under ambient conditions. Chemical Communications, 2019, 55, 14111-14114.	2.2	46
24	Proximity ligation assay induced and DNAzyme powered DNA motor for fluorescent detection of thrombin. Spectrochimica Acta - Part A: Molecular and Biomolecular Spectroscopy, 2019, 207, 39-45.	2.0	17
25	Visualization of silica dispersion states in silicone rubber by fluorescent labeling. Journal of Materials Science, 2019, 54, 5149-5159.	1.7	14
26	A catalytic cleavage strategy for fluorometric determination of Hg(II) based on the use of a Mg(II)-dependent split DNAzyme and hairpins conjugated to gold nanoparticles. Mikrochimica Acta, 2018, 185, 457.	2.5	8
27	Crystal structure and electrochemical properties of [Ni(bztmpen)(CH ₃ CN)](BF ₄) ₂ {bztmpen is <i>N</i> -benzyl- <i>N</i> , <i>N</i> ′, <i>N</i> ′-tris[(6-methylpyridin-2-yl)methyl]ethane-1,2-diamine}. Acta Crystallographica Section E: Crystallographic Communications. 2017, 73, 825-828.	0.2	0
28	Characterization of a trinuclear ruthenium species in catalytic water oxidation by Ru(bda)(pic) ₂ in neutral media. Chemical Communications, 2016, 52, 8619-8622.	2.2	36
29	Nickel Complex with Internal Bases as Efficient Molecular Catalyst for Photochemical H ₂ Production. ChemSusChem, 2014, 7, 2889-2897.	3.6	18
30	A super-efficient cobalt catalyst for electrochemical hydrogen production from neutral water with 80 mV overpotential. Energy and Environmental Science, 2014, 7, 329-334.	15.6	121
31	The influence of a S-to-S bridge in diiron dithiolate models on the oxidation reaction: a mimic of the Hairox state of [FeFe]-hydrogenases. Chemical Communications, 2014, 50, 9255-9258.	2.2	15
32	Redox Reactions of [FeFe]-Hydrogenase Models Containing an Internal Amine and a Pendant Phosphine. Inorganic Chemistry, 2014, 53, 1555-1561.	1.9	24
33	Reactions of [FeFe]-hydrogenase models involving the formation of hydrides related to proton reduction and hydrogen oxidation. Dalton Transactions, 2013, 42, 12059.	1.6	104
34	Electrocatalytic hydrogen evolution from neutral water by molecular cobalt tripyridine–diamine complexes. Chemical Communications, 2013, 49, 9455.	2.2	91
35	Tetranuclear Iron Complexes Bearing Benzenetetrathiolate Bridges as Four-Electron Transformation Templates and Their Electrocatalytic Properties for Proton Reduction. Inorganic Chemistry, 2013, 52, 1798-1806.	1.9	31
	$[\hat{1}]/2$ (Methyleylfanyl)hanzana 1.2 dithialata 1:2 ¹⁰ cuns 4 days di Schistic di Schistic Chistic Colis di Schistic Chistic Colis de	ricarhand	iron(I)]

Lin Chen

#	Article	IF	CITATIONS
37	Simple Nickelâ€Based Catalyst Systems Combined With Graphitic Carbon Nitride for Stable Photocatalytic Hydrogen Production in Water. ChemSusChem, 2012, 5, 2133-2138.	3.6	126
38	Recent progress in electrochemical hydrogen production with earth-abundant metal complexes as catalysts. Energy and Environmental Science, 2012, 5, 6763.	15.6	474
39	Multielectronâ€Transfer Templates via Consecutive Twoâ€Electron Transformations: Iron–Sulfur Complexes Relevant to Biological Enzymes. Chemistry - A European Journal, 2012, 18, 13968-13973.	1.7	31
40	Photocatalytic Water Reduction and Study of the Formation of Fe ^I Fe ^O Species in Diiron Catalyst Sytems. ChemSusChem, 2012, 5, 913-919.	3.6	42
41	Approaches to efficient molecular catalyst systems for photochemical H2 production using [FeFe]-hydrogenase active site mimics. Dalton Transactions, 2011, 40, 12793.	1.6	116
42	Highly Efficient Oxidation of Water by a Molecular Catalyst Immobilized on Carbon Nanotubes. Angewandte Chemie - International Edition, 2011, 50, 12276-12279.	7.2	193
43	Preparation, Facile Deprotonation, and Rapid H/D Exchange of the μ-Hydride Diiron Model Complexes of the [FeFe]-Hydrogenase Containing a Pendant Amine in a Chelating Diphosphine Ligand. Inorganic Chemistry, 2009, 48, 11551-11558.	1.9	84
44	Structures, protonation, and electrochemical properties of diiron dithiolate complexes containing pyridyl-phosphine ligands. Dalton Transactions, 2009, , 1919.	1.6	61
45	[FeFe]-Hydrogenase active site models with relatively low reduction potentials: Diiron dithiolate complexes containing rigid bridges. Journal of Inorganic Biochemistry, 2008, 102, 952-959.	1.5	16
46	Supramolecular self-assembly of a [2Fe2S] complex with a hydrophilic phosphine ligand. CrystEngComm, 2008, 10, 267-269.	1.3	18
47	Multipleâ€Site Concerted Protonâ~'Electron Transfer in a Manganeseâ€Based Complete Functional Model for the [FeFe]â€Hydrogenase. Angewandte Chemie, 0, , .	1.6	2